SIMULATION OF FLOW AND HEAT TRANSFER CHARACTERISTICS OF LAMINATED TURBINE BLADES WITH KEROSENE COOLING CHANNELS

by

Min ZUO[a], Zhen-Zong HE[a,b*], Shi-Jie SUN[a], Jun-Kui MAO[a], and Chuan-Hui DONG[c]

[a] College of Energy and Power Engineering,
Nanjing University of Aeronautics and Astronautics, Nanjing, China
[b] Collaborative Innovation Center for Advanced Aero-Engine, Beijing, China
[c] Shanghai Aircraft Design and Research Institute, Shanghai, China

Original scientific paper
https://doi.org/10.2298/TSCI230115082Z

An air-kerosene thermal mass coupled turbine blade with kerosene micro-channels added to the traditional laminated structure turbine blade is proposed, and numerical simulations are carried out. The enhanced heat transfer mechanism of the air-kerosene thermal mass coupled turbine blade is studied, and the influence of different kerosene temperatures, blowing ratios, and solid thermal conductivity on the heat transfer of the laminated turbine blades is analyzed. The results show that adding kerosene micro-channels can significantly reduce the blade temperature and change the cooling gas heat transfer direction inside the laminate cooling structure. Compared with the traditional laminate cooling structure, adding kerosene micro-channels can significantly improve the heat transfer performance of the blades, and the integrated cooling efficiency increases by 31.7%. Moreover, when the kerosene temperature decreases from 400-300 K, the cooling efficiency increases by 3.9%. Similar conclusions can be obtained by studying the increases in the blowing ratio and the solid thermal conductivity, respectively.

Key words*: turbine blade, aviation kerosene, thermal mass coupling, flow heat transfer*

Introduction

With the development of next-generation high thrust-to-weight ratio aero engines, the challenges faced by high temperature components such as combustion chambers and turbines within aero engines have become increasingly severe. With the limited amount of cooling gas, it is necessary to ensure both the increase in turbine inlet temperature and the increase in engine thrust-to-weight ratio. Therefore, it is particularly important to develop a more efficient turbine blade cooling structure [1]. To achieve a more efficient turbine blade cooling scheme, there are two ideas: one is to develop a new cooling structure, such as a laminated cooling configuration, and the other is to introduce aviation kerosene, which is widely used in aero engines. Laminate cooling is a composite cooling structure that integrates impingement, turbulence, and film cooling. According to the early evaluation report, compared with the traditional cooling configuration, the overall cooling efficiency of the laminated cooling structure can reach 0.7 and the use of cooling air can be reduced by about 40% [2, 3]. Due to its highly integrated structural

* Corresponding author, e-mail: hezhenzong@nuaa.edu.cn

characteristics, the laminate cooling structure involves very complex flow and heat transfer processes. Therefore, the flow and heat transfer characteristics and structural optimization design of laminate cooling structures have become a common concern of researchers in recent decades. Nakamata *et al.* [4] studied the laminated structure's internal heat transfer and external flow characteristics through experiments and numerical simulations, respectively. They believe that the arrangement of the pin fin has an important impact on the internal heat transfer characteristics and the external film cooling efficiency. Li *et al.* [5] numerically simulated the heat transfer characteristics of laminate structures with different pin fin shapes and found that the teardrop-shaped pin fin has better results. Liu *et al.* [6] investigated the overall cooling effect of a composite cooling structure with impingement and effusion and verified it with numerical simulations. The results demonstrate the matching principle. Zhang *et al.* [7] have also carried out relevant studies in the area of turbine blade cooling structures. In addition, the numerical solution of conjugate heat transfer has also been explored [8-10]. In order to identify more efficient cooling structures or solution methods, these studies thoroughly examined the flow heat transfer mechanisms in various laminar structures.

In addition adopting laminate cooling, the regenerative cooling technology that arranges kerosene micro-channels on the outer surface of the engine to reduce the temperature of the external surface of the engine is also one of the future research directions [11]. Aviation kerosene has the advantages of a high heat sink, a strong heat absorption capacity per unit volume, and easy availability in aviation engines. Take JP-8 as an example. The 1 kg of this aviation kerosene is heated from 298-800 K, and the heat absorption is as high as about 1600 kJ, while the heat absorption of the same mass of air is only about 507 kJ for the same temperature increase [12, 13]. Jiang *et al.* [14] used numerical simulations to compare hydrocarbon fuels' flow and heat transfer characteristics in parallel channels with four different cross-sectional shapes at supercritical pressure. Li *et al.* [15] also investigated the heat transfer enhancement and heat transfer deterioration of hydrocarbon fuels in spiral and rectangular cooling channels at supercritical pressure.

In summary, the aforementioned studies focus on the effect of different laminate structures on the flow characteristics and the heat transfer mechanism. Or the flow heat transfer behavior of hydrocarbon fuels. Few existing studies have considered kerosene micro-channels and the laminate cooling structure together. Therefore, based on conventional cooling structures, it is particularly important to develop new cooling structures by taking advantage of the high heat sink characteristics of aviation kerosene. This paper proposes an air kerosene thermally mass-coupled turbine blade with kerosene micro-channels. A numerical simulation method is also used to investigate the flow heat transfer characteristics of the air kerosene thermal mass coupled turbine blade. The effects of different kerosene temperatures, blowing ratios, and solid thermal conductivity on their heat transfer performance was also analyzed, thus providing a new idea for designing future turbine blade cooling structures.

Numerical methods

Physical model

The physical model studied in this paper is shown in fig. 1, and a cooling channel in the middle region of the turbine blade chord length is selected. The inlet and outlet of this laminate structure are one row of impingement holes and three rows of film holes, respectively, and three rows of pin fins in the cavity. The impingement holes, the pin fins, and the film holes are arranged in a row. Due to the small curvature of individual cooling units, the model is simplified to a laminate model. Also, considering its structure's periodicity and flow similarity, the red region shown in fig. 1 was selected as the study object.

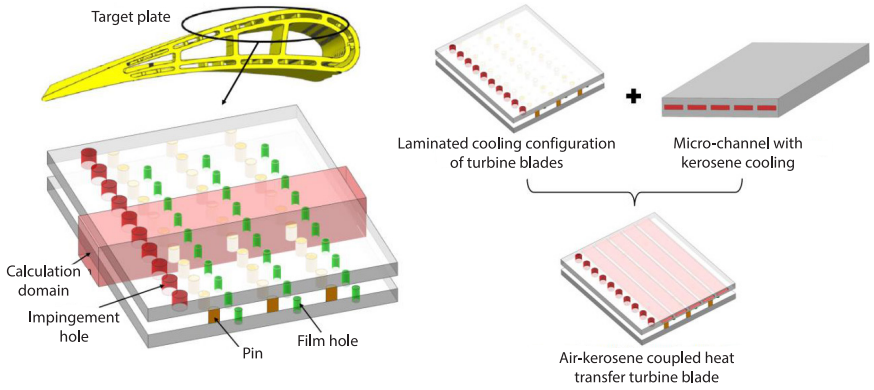

Figure 1. Air-kerosene thermal mass coupled heat transfer turbine blade structure

Boundary conditions

The numerical mode boundary conditions for the computational domain are given in fig. 2, with detailed parameters according to [6]. The main flow, coolant inlet and kerosene channel inlet are defined as mass inlet boundary:

$$\rho_g u_g A_g = \dot{m}_g \tag{1}$$

$$\rho_c u_c A_c = \dot{m}_c \tag{2}$$

$$\rho_k u_k A_k = \dot{m}_k \tag{3}$$

where u_g = 216 m/s, T_g = 1666 K . The coolant inlet parameters are calculated from the blowing ratio.

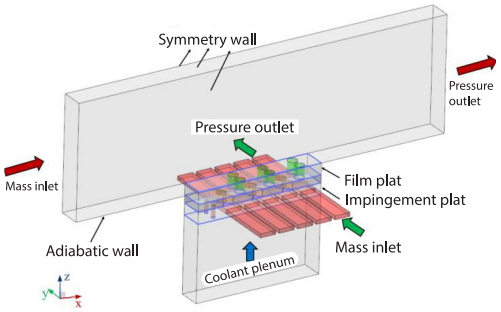

Figure 2. Computation model boundary condition setting

For the kerosene channel, $\dot{m}_k$ = 3 g/s in a single channel. The symmetric boundary conditions are used on both sides of the main and secondary flow channels and on the upper side of the main flow channel. The rest of the surfaces are set to no-slip adiabatic boundary conditions.

Mesh and validation

The software FLUENT MESHING was used to mesh the computational model, as shown in fig. 3, and the mesh was locally encrypted near the laminate structure. A boundary-layer was set in the near-wall region of the fluid-solid contact, with the first mesh height set to 0.001 mm and the growth rate to 1.1 for 15 layers. Before performing formal calculations, grid-independence verification was performed. The computational domain was solved using FLUENT software. The turbulence model and the detailed settings are discussed in detail in section *Model validation*. The average temperature on the gas film side, the average temperature inside the laminate, and the average temperature at the kerosene outlet were investigated as a relationship with the number of grids, as shown in fig. 4. As can be seen from the figure, when the number of grids reaches 5.52 million, the impact of continuously increasing the number of grids on the evaluation index gradually decreases, and the change rate is less than 1%. Therefore, to balance computational resources and accuracy, 5.52 million grids were selected for all subsequent studies.

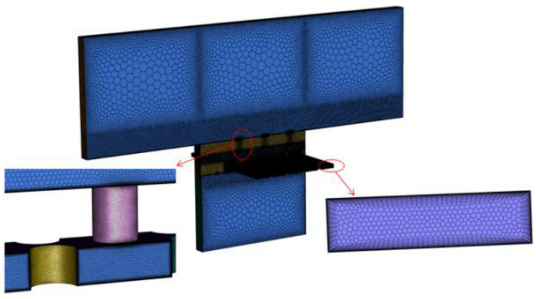

Figure 3. Computational domain mesh

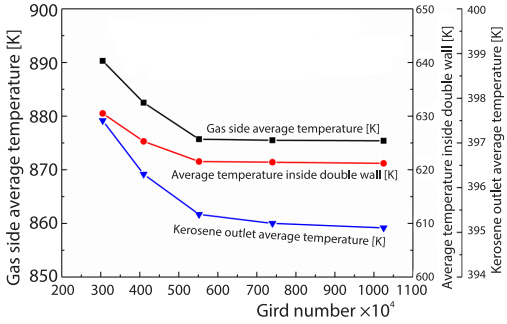

Figure 4. Grid independence verification

Model validation

These geometric parameters and boundary conditions, according to the experimental model of Jung *et al.* [16], were studied to verify the turbulence model. From fig. 5(a), the numerical calculation of the SST *k-ω* turbulence model is closest to the experimental value. The maximum error is less than 5%, much smaller than the other models. From fig. 5(b), the SST *k-ω* turbulence model has high computational accuracy at different Biot numbers based on the mainstream gas. Furthermore, Dees *et al.* [17], Mensch *et al.* [18], Gomatam and Shih [19], Zhou *et al.* [20], and Dyson *et al.* [21] demonstrated that the SST *k-ω* turbulence model can accurately predict the flow and heat transfer of the laminate cooling structure. As a result, the SST *k-ω* turbulence model is used to simulate all of the calculation models in this paper numerically, and the wall function is chosen as the enhanced wall function. The second-order upwind format solves the problem of turbulent kinetic energy, momentum, density, turbulent dissipation rate, and energy. The residuals of each solution are set as 10^{-6}.

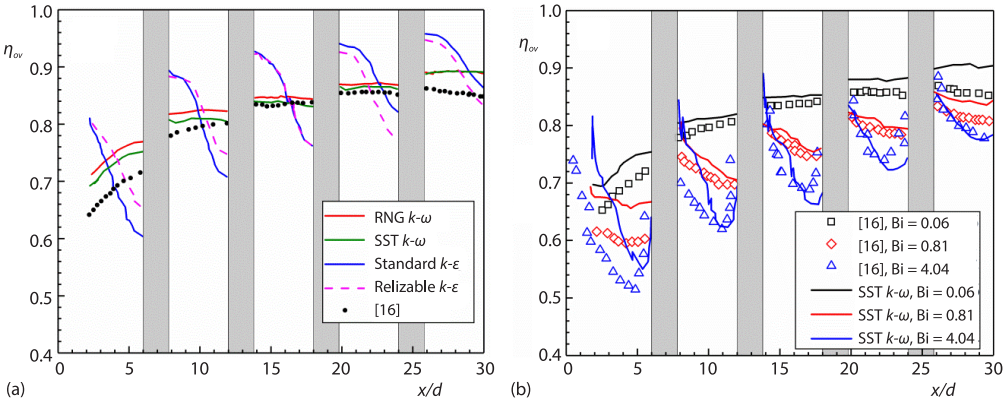

Figure 5. Numerical model validation; (a) local comprehensive cooling efficiency (y/d = 1.5) and (b) local comprehensive cooling efficiency for different Biot numbers (y/d = 1.5)

Results and discussions

Parameter definition

– Comprehensive cooling efficiency

The comprehensive cooling efficiency is a dimensionless parameter to reflect the temperature distribution on the coupling wall of the blade film side:

$$\eta_{ov} = \frac{T_g - T_{wg}}{T_g - T_c} \tag{4}$$

where T_g and T_c are the temperatures of the mainstream and secondary flow gases, respectively, and T_{wg} is the temperature on the coupling wall of the blade film side.

– The blowing ratio:

$$M = \frac{\rho_c u_c}{\rho_g u_g} \tag{5}$$

where M is the blowing ratio, ρ_c and u_c are the density and velocity of the secondary stream cold gas, and ρ_g and u_g – the density and velocity of the mainstream gas, respectively.

– Nusselt number:

$$\mathrm{Nu} = \frac{hd}{\lambda} \tag{6}$$

where h is the convective heat transfer coefficient and d and λ are the equivalent diameter and thermal conductivity, respectively.

Analysis of enhanced heat transfer mechanism

The effect of kerosene micro-channels on the heat transfer characteristics of the laminate cooling structure was investigated under working conditions of a blowing ratio of 1, a solid thermal conductivity of 23.2 W/mK, and a kerosene inlet temperature of 300 K.

In the laminate cooling structure, the temperature of the cooling gas is very important. On the one hand, increasing the cooling gas temperature reduces its internal cooling efficiency. On the other hand, a higher film outlet temperature tends to reduce the efficiency of film cooling on the gas side. Figure 6 compares the cooling gas temperatures for the laminate cooling structure with and without kerosene micro-channels. As shown in fig. 6(a), the temperature of the cooling gas inside the laminate cooling structure is highly uneven due to the heating of the high temperature heat flow from the gas side, as well as the convection and impact cooling effects of the cooling gas in the interior. It is mainly reflected in the relatively low temperature near the impingement hole, and the temperature gradually increases as the cooling gas progresses downstream and the absorbed heat increases. A large area of a high temperature region is formed near the third film hole. On the cooling side, the cooling air will form a local high tem-

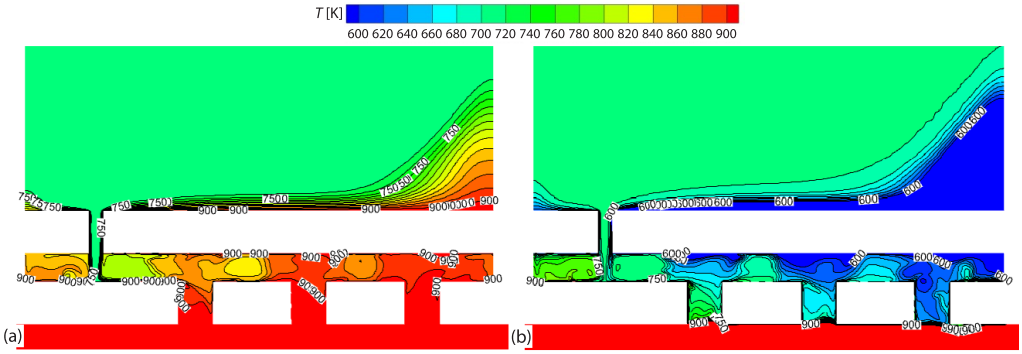

Figure 6. Comparison of cooling gas temperature of laminate cooling structure with and without kerosene micro-channels; (a) without kerosene microchannel and (b) with kerosene microchannel

perature zone at the trailing edge due to the influence of the trailing edge vortex and solid heat conduction. The presence of the high temperature areas will reduce the heat exchange at the blade's trailing edge, resulting in high temperatures. It is clear from fig. 6(b) that all of the high temperature regions in the structure's interior and the trailing edge part of the cooling gas side have greatly improved. In particular, above each film hole and at the trailing edge of the cold air side, the maximum cooling gas temperature reduction reaches about 300 K. This indicates that the addition of kerosene micro-channels in the laminate cooling structure can significantly reduce the cooling air temperature and realize the transition from a gradual temperature increase to a temperature decrease during the cooling air downstream.

Figure 7 compares the solid domain temperature of the laminate cooling structure. It can be found that the temperature of the solid domain decreases significantly after the addition of the kerosene micro-channel. The maximum temperature of the solids on the gas side decreases by about 230 K . It reaches a minimum of about 750 K. The maximum temperature of the solids on the cooling gas side decreases by about 510 K. It reaches a minimum of about 390 K. In the laminate cooling structure without kerosene micro-channels, the temperature of the cooling air side and gas side of the blade is higher than the temperature of the cold air inlet. Hence, the cooling gas absorbs heat from both sides, as shown in fig. 8. In the laminate cooling structure with kerosene micro-channels, the temperature of the cooling side of the blade will be greatly reduced because the kerosene absorbs part of the heat.

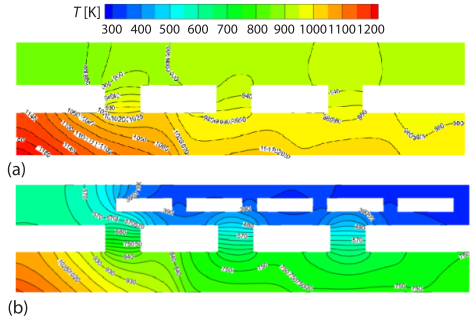

Figure 7. Comparison of the solid domain temperature with and without kerosene micro-channels

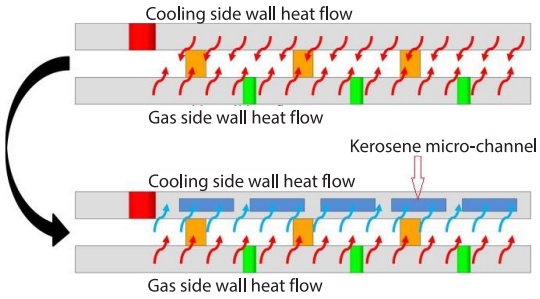

Figure 8. Schematic diagram of temperature transfer of cooling gas inside the laminate cooling structure

The Nusselt number distribution inside the laminate cooling structure with and without kerosene micro-channels is given in fig. 9. The Nusselt number is calculated with the inlet temperature of kerosene at 300 K as the reference. After introducing kerosene micro-channels, the surface Nusselt number of the first row of pins decreases along the cooling gas-flow direction. However, those of the second and third rows of pins increase significantly. The increase in the solid wall Nusselt number allows the metal solid to carry away more heat from the cooling air, which is one of the important reasons why the addition of kerosene micro-channels can reduce the cooling air above each film hole extremely significantly. As noted in tab. 1, adding kerosene micro-channels enhanced the heat transfer of the laminate cooling structure by about 14%. It is worth mentioning that the heat exchange is improved by 274.89% on the cooling gas side wall. This change substantially improves the heat exchange of the cooling gas side wall to reach or surpass that of the gas side wall, which also makes full use of the huge heat exchange area of the cooling gas side wall. By comparing the changes in heat transfer in the walls of the three rows of pin fins and film holes, it can be found that the heat transfer in the walls of the

second and third rows of pin fins and film holes has increased in different magnitudes due to the decrease in cooling gas temperature, which also indicates that the decrease in cooling gas temperature significantly increases the heat transfer inside the laminate cooling structure.

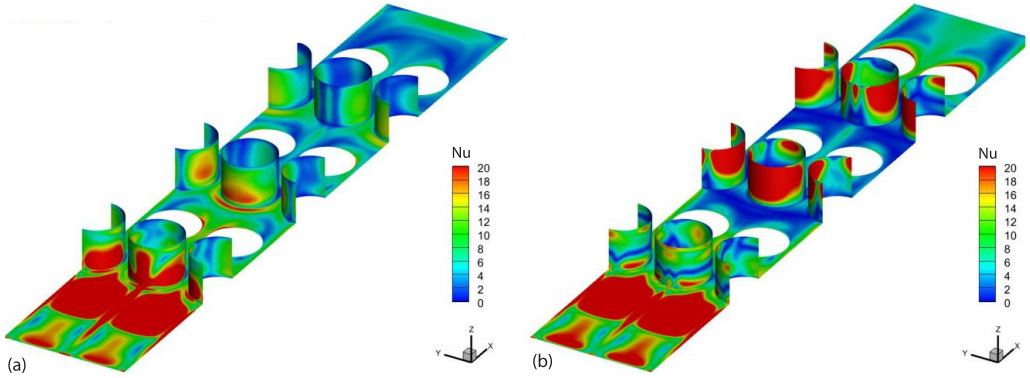

Figure 9. Nusselt number distribution within the laminate cooling structure with and without kerosene micro-channels; (a) without kerosene microchannel and (b) with kerosene microchannel

Table 1. Comparison of heat exchange between the internal surface of the laminate cooling structure with and without kerosene micro-channel

Area	Without kerosene micro-channel [W]	With kerosene micro-channel [W]	Change value [%]
Impingement hole	0.86	1.17	36.26
Cooling side wall surface	2.97	11.13	274.89
Gas side wall surface	12.51	9.28	–25.83
First row of pin fins	2.69	0.27	–89.96
Second row of pin fins	1.41	1.54	9.34
Third row of pin fins	1.08	1.71	58.32
First row of film hole	2.03	1.49	–26.46
Second row of film hole	0.84	1.08	28.02
Third row of film hole	1.04	1.31	26.27
Total	25.42	28.98	14.00

Figure 10 compares the integrated cooling efficiency of the laminate cooling structure and without kerosene micro-channels. The kerosene micro-channel structure can substantially improve the integrated cooling efficiency of the blade surface. Figure 11 compares the average combined cooling efficiency of the two along the blade surface in the flow direction. The structure with kerosene micro-channels has a greater increase in the combined cooling efficiency behind the film holes. In the vicinity of the blade leading edge impingement hole, the integrated cooling efficiency of the blade surface is improved by about 15-20%, while the integrated cooling efficiency of the blade surface behind the blade film hole is improved by about 30-40%. Compared to the average integrated cooling efficiency of the two structures, the structure without kerosene micro-channels had a cooling efficiency of only 0.6305. In contrast, the average integrated cooling efficiency of the structure's surface with kerosene micro-channels reached 0.8275, an improvement of 31.2%.

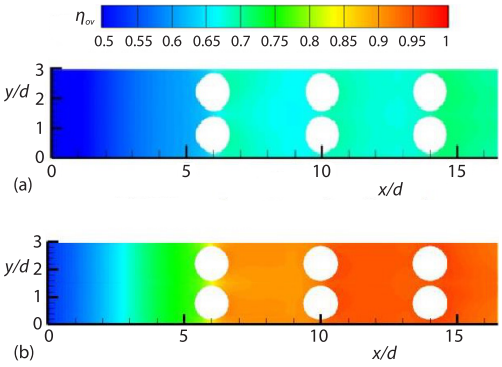

Figure 10. Comparison of the integrated cooling efficiency of the laminate cooling structure with and without kerosene micro-channels; (a) without kerosene microchannel and (b) with kerosene microchannel

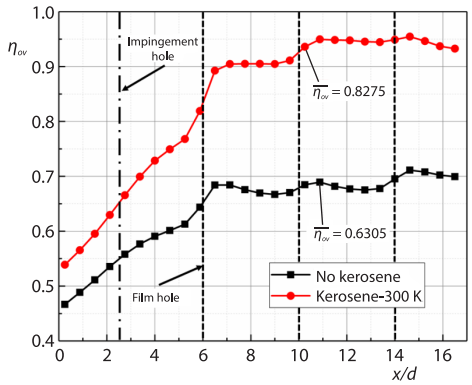

Figure 11. Average integrated cooling efficiency of flow direction of the laminate cooling structure with and without kerosene micro-channels

Effect of kerosene temperature on integrated cooling efficiency

Figure 12 compares the integrated cooling efficiency distribution at different kerosene temperatures. It can be seen that the change in the integrated cooling efficiency on the blade surface is small when the kerosene temperature is reduced from 400-300 K. The change is slightly larger behind each film hole. The average integrated cooling efficiency at different kerosene temperatures is shown in fig. 13. The average integrated cooling efficiency will increase by 3.9% when the kerosene temperature reduces by 25%. Therefore, it can be seen that the effect of kerosene temperature variation on the integrated cooling efficiency of the blade surface is small, which also indicates that the addition of kerosene channels does not aggravate the temperature inhomogeneity of the blade surface in the actual blade.

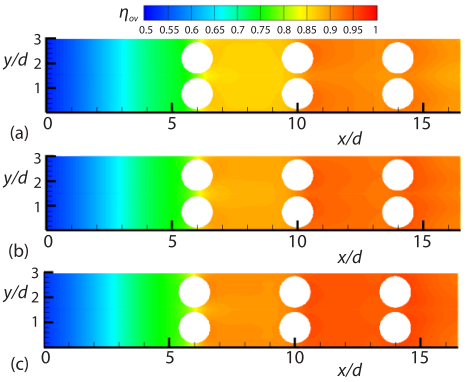

Figure 12. Distribution of integrated cooling efficiency at different kerosene temperatures; (a) T_k = 400 K and (b) T_k = 350 K, (c) T_k = 300 K

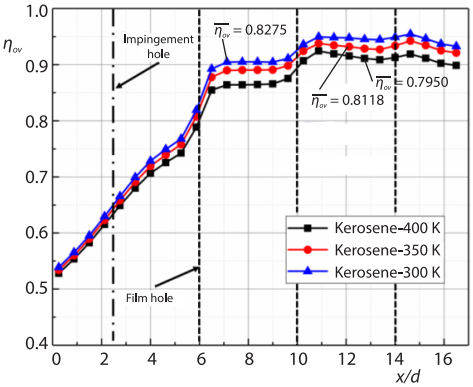

Figure 13. Comparison of average integrated cooling efficiency of flow direction at different kerosene temperatures

Effect of blowing ratio on integrated cooling efficiency

Figure 14 gives a comparison of the integrated cooling efficiency distribution for different blowing ratios. When the blowing ratio increases from 0.5-1.5, the integrated cooling efficiency of the blade surface increases significantly, especially in the area behind the leading edge of the blade and each film hole. Figure 15 compares the average integrated cooling efficiency of the flow direction of the laminate cooling structure with and without kerosene micro-channels for different blowing ratios. In both structures, the average integrated cooling efficiency of the blade surface flow shows a tendency to increase with the blowing ratio. It is worth mentioning that in the structure with kerosene micro-channels at a blowing ratio of 0.5, the integrated cooling efficiency has surpassed the structure's integrated cooling efficiency without kerosene micro-channels at a blowing ratio of 1.5. The advantage is that the laminate cooling structure with kerosene micro-channels can achieve the required cooling efficiency in actual engine operation with less cooling gas, thus further increasing the engine thrust-to-weight ratio. When the blowing ratio increases from 0.5-1.5, the area average integrated cooling efficiency increases by 16.22%.

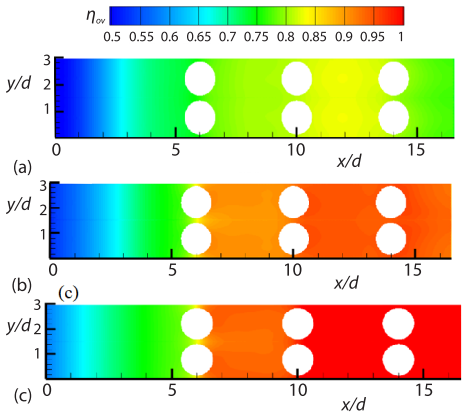

Figure 14. Distribution of integrated cooling efficiency; (a) M = 0.5, (b) M = 1.0, and (c) M = 1.5

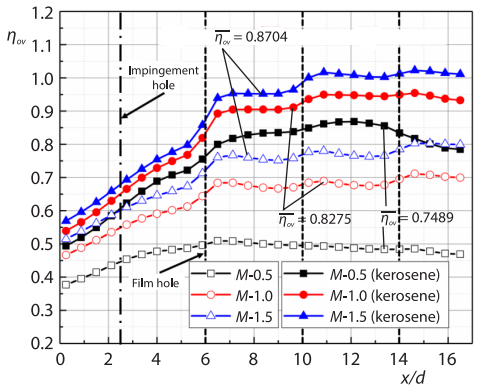

Figure 15. Comparison of the average integrated cooling efficiency

Effect of thermal conductivity of solid domain on integrated cooling efficiency

Figure 16 shows the integrated cooling efficiency distribution under different thermal conductivity coefficients. The integrated cooling efficiency is relatively small when the thermal conductivity is 1.7 W/mK. Only a localized high efficiency area appears at the rear position of the three exhaust film holes, resulting in a very uneven distribution of comprehensive cooling efficiency. When the thermal conductivity rises to 23.2 W/mK, the integrated cooling efficiency and the unevenness decrease, the integrated cooling efficiency of the blade surface is regionally consistent, and all remain at a high level when the thermal conductivity is increased to 298 W/mK. The average integrated cooling efficiency in the flow direction for different thermal conductivities is compared in fig. 17. The integrated cooling efficiency of the blade surface is only 0.1 at the blade's leading edge when the thermal conductivity is 1.7 W/mK. At the same time, the integrated cooling efficiency of the blade surface decreases abruptly after each film hole. When the thermal conductivity reaches 298 W/mK, the integrated cooling efficiency of

the blade surface from the leading edge to the trailing edge exceeds 1.0 and reaches 1.21 at the highest. The cooling efficiency has changed by 119.64%.

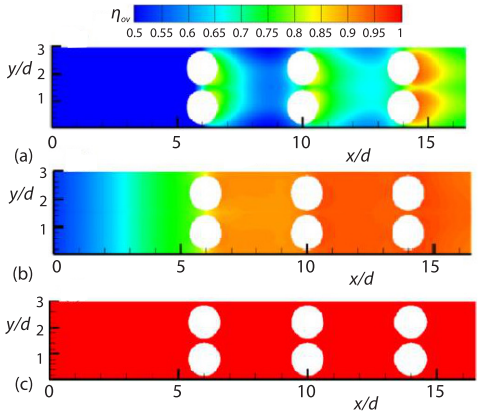

Figure 16. Distribution of integrated cooling efficiency under different heat conductivity; (a) λ = 1.7 W/mK, (b) λ = 23.2 W/mK, (c) λ = 298 W/mK

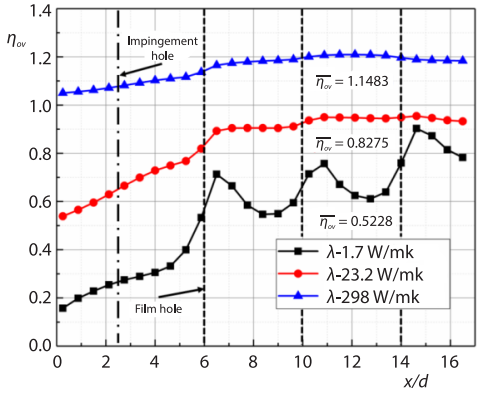

Figure 17. Comparison of average integrated cooling efficiency of flow direction with different thermal conductivity

Conclusions

In this paper, an air-kerosene thermal mass coupled turbine blade with kerosene micro-channels arranged on the conventional laminate cooling structure turbine blade is proposed, and its enhanced heat transfer mechanism is investigated. The effects of different kerosene temperatures, blowing ratios, and solid thermal conductivity on its heat transfer performance are also analyzed, and the specific conclusions are as follows.

- The addition of kerosene micro-channels has a great influence on the heat transfer characteristics of the traditional turbine blade laminate cooling structure. Compared with the structure without kerosene micro-channels, introducing kerosene micro-channels can significantly improve the integrated cooling efficiency behind the air film pores on the blade surface and increase the average integrated cooling efficiency of the blade surface area by 31.7%.
- As the kerosene temperature increases, the average integrated cooling efficiency of the blade area decreases. When the kerosene temperature increased from 300-400 °C, the average integrated cooling efficiency decreased by 3.9%.
- As the blowing ratio decreases, the average integrated cooling efficiency of the blade area increases. When the blowing ratio increased from 0.5-1.5, the average integrated cooling efficiency increased by 16.22%.
- As the blade's thermal conductivity increases, the average cooling efficiency of the blade increases. The increase in thermal conductivity can improve the problem of non-uniformity in cooling efficiency distribution. When the solid thermal conductivity increased from 1.7-298 W/mK, the area average integrated cooling efficiency increased by 119.64%.

Acknowledgment

The supports of this work by the National Natural Science Foundation of China (No. 51806103, 52206090), the Fundamental Research Funds for the Central Universities and

the China Postdoctoral Science Foundation (No. 2022TQ0149), and they are gratefully acknowledged. A very special acknowledgment is made to the editors and referees who make important comments to improve this paper.

Nomenclature

d – equivalent diameter, [m]
h – convective heat transfer coefficient, [$Wm^{-2}K^{-1}$]
M – blowing ratio
$\dot{m}$ – mass-flow rate, [kgs^{-1}]
Nu – Nusselt number
T – temperature, [K]
u – velocity, [ms^{-1}]

Greek symbols

η_{ov} – integrated cooling efficiency
λ – thermal conductivity, [$Wm^{-1}K^{-1}$]
ρ – density, [kgm^{-3}]

Subscripts

c – cooling gas
g – mainstream gas
k – kerosene
wg – coupling wall of the blade

References

[1] Peters, J. E., Current Gas Turbine Combustion and Fuels Research and Development, *Proceedings*, ASME 1987 International Gas Turbine Conference and Exhibition, Volume 3: Coal, Biomass and Alternative Fuels; Combustion and Fuels; Oil and Gas Applications; Cycle Innovations, Anaheim, Cal., USA, 1987
[2] Nealy, D. A., Evaluation of Laminated Porous Wall Materials Combustor Liner Cooling, *Proceedings*, Gas Turbine Conference and Exhibit and Solar Energy Conference, San Diego, Cal., USA, 1979, p. 9
[3] Wang, C. H., *et al*., Modelling and Performance Evaluation of a Novel Passive Thermoelectric System Based on Radiative Cooling and Solar Heating for 24-Hour Power-Generation, *Applied Energy*, *331* (2023), 120425
[4] Nakamata, C., *et al*., Spatial Arrangement Dependance of Cooling Performance of an Integrated Impingement and Pin Fin Cooling Configuration, *Proceedings*, ASME Turbo Expo 2005: Power for Land, Sea, and Air, Turbo Expo 2005, Parts A and B, Reno, Nev., USA, 2005, Vol. 3, pp. 385-395
[5] Li, L., *et al*., Influence of Pin Shape on Heat Transfer Characteristics of Laminated Cooling Configuration, *Proceedings*, ASME Turbo Expo 2019: Turbomachinery Technical Conference and Exposition, Heat Transfer, Phoenix, Ariz., USA, 2019, Vol. 5B
[6] Liu, C. L., *et al*., Study on analogy Principle of Overall Cooling Effectiveness For Composite Cooling Structures with Impingement and Effusion, *International Journal of Heat and Mass Transfer*, *127* (2018), Part B, pp. 639-650
[7] Zhang, B., *et al.*, Experimental investigation of Geometrical Effect on Flow and Heat Transfer Performance of Lamilloy Cooling Structure, *Thermal Science*, *24* (2020), 3A, pp. 1835-1843
[8] Ren Y. T., *et al.*, Passive control of Temperature Distribution in Cancerous Tissue during Photo-Thermal Therapy Using Optical Phase Change Nanomaterials, *International Journal of Thermal Sciences*, *161* (2021), 106754
[9] Liu, Y., *et al*., Numerical and Experimental Investigationg of a Turbine Guide Vane with Conjugate Heat Transfer Method, *Thermal Science*, *26* (2022), 5B, pp. 4259-4269
[10] Yang, J., *et al.*, Numerical simulations and optimizations for turbine-related configurations, *Thermal Science*, *24* (2020), 1A, pp. 367-378
[11] Zhang, S., *et al*., Review on Regenerative Cooling Technology of Hypersonic Propulsion, *Journal of Propulsion Technology, 39* (2018), 10, pp. 2177-2190
[12] Chin, J., Lefebvre, A. H., Experimental techniques for the Assessment of Fuel Thermal Stability, *Journal of Propulsion and Power*, *8* (1992), 6, pp. 1152-1156
[13] He, M. J., *et al*., Micro/Nanomaterials for Heat Transfer, Energy Storage and Conversion, *Coatings*, *13* (2022), 11
[14] Jiang, Y., *et al*., The Flow Rate Distribution of Hydrocarbon Fuel in Parallel Channels with Different Cross-Section Shapes, *Applied Thermal Engineering*, *137* (2018), June, pp. 173-183
[15] Li, N., *et al.*, Effects of Channel Geometries and Acceleration on Heat Transfer of Hydrocarbon Fuel, *Journal of Thermophysics and Heat Transfer, 34* (2020), 3, pp. 570-578
[16] Jung, E. Y., *et al*., Conjugate Heat Transfer on Full-Coverage Film Cooling with Array Jet Impingements with Various Biot Numbers, *Experimental Thermal and Fluid Science*, *83* (2017), May, pp. 1-8

[17] Dees, J. E., *et al*., Experimental Measurements and Computational Predictions for an Internally Cooled Simulated Turbine Vane, *Journal of Turbomachinery*, *134* (2012), 6, 061003
[18] Mensch, A., *et al*., Conjugate heat Transfer Measurements and Predictions of a Blade Endwall With a Thermal Barrier Coating, *Journal of Turbomachinery*, *136* (2014), 12, 121003
[19] Gomatam, S., Shih., T. I., Biot number Analogy for Design of Experiments in Turbine Cooling, *Journal of Turbomachinery*, *137* (2015), 6, 061002
[20] Zhou, W., *et al.*, Conjugate Heat Transfer Analysis for Laminated Cooling Effectiveness – Part A: Effects of Surface Curvature, *Proceedings*, ASME Turbo Expo 2016: Turbomachinery Technical Conference and Exposition, Heat Transfer, Seoul, South Korea, 2016, Vol. 5A
[21] Dyson, T. E., *et al*., Evaluation of CFD simulations 0f Film Cooling Performance on a Turbine Vane Including Conjugate Heat Transfer Effects, *International Journal of Heat and Fluid-Flow*, *50* (2014), Dec., pp. 279-286

Paper submitted: January 15, 2023
Paper revised: February 23, 2023
Paper accepted: February 27, 2023